Assessing field-scale variability of soil hydraulic conductivity at and near saturation

Xi Zhang*, Ole Wendroth, Christopher Matocha, Junfeng Zhu, Javier Reyes

Author affiliations

Xi Zhang, Ole Wendroth, Christopher Matocha, Dep. of Plant and Soil Sciences, Univ. of Kentucky, Lexington, KY 40546; Junfeng Zhu, Kentucky Geological Survey, Univ. of Kentucky, Lexington, KY 40506; Javier Reyes, Dep. of Soil System Science, Helmholtz-Centre for Environmental Research-UFZ, Leipzig, Germany 04318.

* Corresponding author (xi.zhang@uky.edu)

Highlights

1. Spatial variation of $K(h)$ in a field was characterized in its relationship to EC_a.

2. Spatial variability of K_s was caused to some degree by macropore effects.

3. Field scale $K(h)$ mapping using PTFs should be handled with caution.

Abstract

Saturated hydraulic conductivity (K_s) is a crucial hydraulic property for assessing soil water dynamics. Understanding the spatial variability of K_s in a field is important for site-specific resource management. However, direct measurement of hydraulic conductivity K as a function of soil water pressure head h [$K(h)$] is time consuming and laborious. Alternatively, pedotransfer functions (PTFs) have been developed to predict K_s indirectly based on more easily measurable soil properties. Although PTFs have been used for decades, their validity for estimating the field-scale spatial variability of K_s remains unclear. The objectives of this study were to characterize the spatial pattern of $K(h)$ at and near saturation in an agricultural field by a coregionalization technique, and in comparison, to evaluate the performance of ROSETTA PTF in characterizing the spatial variability of $K(h)$ at the field scale. Surface soil (7-13 cm) $K(h)$ in the vertical direction was measured at 48 locations in a 71-m by 71-m grid within a no-till farmland. Apparent electrical conductivity was densely measured using a contact sensor Veris 3150 and used as ancillary variable in a coregionalization approach. Experimental semivariograms and cross semivariograms were derived and applied in cokriging to generate $K(h)$ maps. Geostatistical analysis presented similarities in maps of measured $K(h)$ with ROSETTA-predicted $K(h)$ data for a matric potential of -10 cm. However, the strong spatial heterogeneity of measured K_s, which was caused by macropores, observed in the field was not captured by ROSETTA estimates. The results indicated that texture dominated PTFs like ROSETTA, in which soil structure is not considered, might be useful in characterizing the spatial pattern of unsaturated hydraulic conductivity rather than K_s. Field scale K_s maps based on PTF estimates should be evaluated carefully and handled with caution.

Keywords

Hydraulic conductivity, Pedotransfer functions (PTFs), Spatial variability, Coregionalization, Field scale

Abbreviations list

$K(h)$: Hydraulic conductivity; K_s: Saturated hydraulic conductivity; PTFs: Pedotransfer functions; EC_a: Apparent electrical conductivity; RNE: relative nugget effect; S.D.: Standard deviation; K-S: Kolmogorov-Smirnov test.

1. Introduction

Hydraulic conductivity at and near saturation of the soil surface layer plays an important role in partitioning precipitation and irrigation water into surface runoff and soil water, and regulating water transport in the vadose zone (Jarvis et al., 2013; Ugarte Nano et al., 2015; Gadi et al., 2017). Soil saturated hydraulic conductivity (K_s), which determines the maximum rate of soil to transmit water, is a crucial hydraulic parameter for hydrological models (e.g., HYDRUS, RZWQM2) (Mallants et al., 1997; Zhao et al., 2016). In many field soils, K_s is strongly influenced by structural macropores and exhibits high spatial heterogeneity (Jarvis et al., 2002; Strudley et al., 2008). Due to the high spatial variability of K_s, the optimum application rate and amount of irrigation water differs between specific areas within the same field (Al-Karadsheh et al., 2002). Accurate characterization of the spatial variation of K_s at the field scale is therefore important for precision irrigation management and indentifying local management zones (Gumiere et al., 2014). A map of the spatial distribution of K_s can become useful for guiding site-specific irrigation, helping farmers to apply the right amount of water in the right areas at the right intensity while minimizing the environmental risks, e.g., leaching, surface runoff, oxygen deficiency through over-irrigation, and plant-water stress and yield loss through under-irrigation.

Saturated hydraulic conductivity can be measured either in the field with in-situ methods (e.g., borehole infiltrometer, Amoozemeter) or in the laboratory with a permeameter (Klute and Dirksen, 1986; Amoozegar, 1989; Stephens, 1992). However, K_s is a parameter that exhibits enormous spatial variability (Nielsen et al., 1973; Schaap and Leij, 1998b). Large numbers of soil samples are generally required to accurately characterize K_s in a study area (Yao et al., 2015). For example, Vieira et al. (1981) characterized the spatial variability of infiltration rate based on 1280 measurements. By comparing different scenarios, they found that at least 128 field-measured values were required in order to obtain useful spatial information in a field with an area of 0.88 ha. Accurate characterization of K_s using direct measurements, therefore, are laborious, time-consuming, and expensive (Li et al., 2007; Wang et al., 2012). To overcome these limitations and to quantify K_s for large regions, alternative approaches have been developed to estimate K_s indirectly through more easily measurable soil properties that may already exist from soil surveys or from existing soil databases (Zhang et al., 2019). Among these alternative approaches, pedotransfer functions (PTFs) are increasingly used to estimate K_s (Wösten et al., 2001; McBratney et al., 2011). In the past decades, the accuracy and reliability of PTFs for estimating K_s have been critically evaluated (Tietje and Hennings, 1996; Schaap and Leij, 1998a; Wagner et al., 2001; Alvarez-Acosta et al., 2012; Yao et al., 2015). The PTF estimate at a single point is usually compared with the measured value at the same location. Although estimation of K_s at a single point is necessary for modeling water flow and solute transport in a soil profile, a detailed description of the spatial variability or distribution of K_s is needed for field water management with distributed hydrological models (Liao et al., 2011). Several authors have studied the spatial characterization of unsaturated hydraulic conductivity (soil water pressure, h, less than -10 cm) by using both measured data and PTF predictions (e.g., Romano, 2004; da Silva et al., 2017), however, far fewer studies investigated the performance of PTFs in describing spatial structure or characterizing spatial patterns of K_s in a field and the results are inconsistent (Springer and Cundy, 1987; Leij et al., 2004). Although PTF estimates revealed stronger spatial dependence than independently measured data and the generated spatial pattern of hydraulic conductivity depended on the choice of PTFs, kriged maps of unsaturated hydraulic conductivity based on measurements and on PTFs estimates showed similarities in their spatial variations. (Romano, 2004; da Silva et al., 2017).

Unsaturated water flow at h < -10 cm mainly takes place in the soil matrix and soil texture places a significant impact on unsaturated hydraulic conductivity (Lin et al., 1999b; Schaap and Leij, 2000). For saturated or near-saturated water flow ($h \geq$ -10 cm), the behavior differs. Hydraulic conductivity at or near saturation is sensitive to even small volume fractions (0.1%-5%) of macropores, which are affected by agricultural management and biological activities (Rienzner and Gandolfi, 2014). Inter-aggregate macropores form the primary pathways for rapid water flow. Water flow through soil is influenced not only by macropores size and shape, but also by their vertical continuity (Bouma et al., 1977). The presence and connectivity of macropores are governed by soil structure. In general, soil with granular structure has high infiltration rate, while block- and prism-like structure has moderate infiltration rate. Platy soil structure impedes water infiltration and encourages lateral flow (Germán Soracco et al., 2010). Thus, soil structure also impacts the anisotropy of K_s. In well-structured soil, water is mostly stored in the intra-aggregate micropores due to the inter-aggregate macropores rapidly drain at the end of infiltration and water slowly redistributes via a network of contacting aggregates (Berli et al., 2008). Soil micropores is determined by texture. Therefore, soil structure is important for saturated and near-saturated water flow, while unsaturated water flow is influenced more by soil texture. In field soils with structural macropores, a large decrease (e.g., several orders of magnitude) in hydraulic conductivity is often observed as water pressure even slightly drops from saturation to near-saturated conditions (-10 cm < h < 0 cm) (Jarvis and Messing, 1995; Jarvis et al., 2002; Braud et al., 2017). Hydraulic conductivity at near saturation, therefore, can be used to identify macropore effects in a field. Although basic soil physical properties (e.g., texture, bulk density, and organic matter) are commonly used as PTF predictors, their influence on K_s is usually masked by macropore effects (Buttle and House, 1997). However, soil structure or macropore information is not included in most published PTFs (Lin et al., 1999b; Weynants et al., 2009; Vereecken et al., 2010). PTFs that relate K_s to basic soil physical properties alone may therefore not accurately estimate K_s for soils with pronounced structural macropores (Lin et al., 1999a).

Since PTF predictors (i.e., basic soil physical properties) can only be sampled for a limited number of points in an area, PTF estimates at these points have to be combined with spatial interpolation to make predictions at unsampled locations with the result that the estimated spatial variability reflects the behavior of the target variable less than the PTF input variables. At each sampled location, the uncertainty (e.g., measurement errors) in the input variables also causes uncertainty in the PTF estimates. This uncertainty is further propagated to the interpolation process and is the larger the farther away an interpolated point is located from the next measured point (Chirico et al., 2007). Moreover, the spatial interpolation of PTF-predicted data is dominated by the spatial variability pattern of the underlying predictors, which may deviate from the spatial variability pattern of measured hydraulic conductivity data, especially if soil structural features affect their magnitude, such as macropores. Springer and Cundy (1987) compared measurements of K_s with predicted data obtained from two published PTFs at the field scale, and the semivariogram of the measured data was well reproduced by one of the PTFs. They also found that the correlation length was shorter for the field-measured data. Leij et al. (2004) did similar work in a field with structural soil, however, their findings were discouraging since all the selected PTFs failed to capture the spatial structure of observed K_s. Furthermore, Pringle et al. (2007) emphasized that PTFs are scale dependent. PTF-estimated data is unable to provide a reasonable portrayal of the spatial variations exhibited by measured data at all spatial scales. These studies indicate that there are still significant uncertainties about whether the spatial variability of K_s observed in a field can be captured by PTF-predicted data. Therefore, characterizing the field-scale spatial pattern of K_s predicted with a PTF still needs to be critically evaluated. To this end, the primary objective of this study was to characterize the spatial variability of hydraulic conductivity at and near saturation in an agricultural field by geostatistical analysis using both measured and PTF estimated data.

2. Materials and Methods

2.1. Site description and soil sampling

This study was conducted in an agricultural field (~30 ha) located in Caldwell County, Kentucky, United States (37°1′42″-37°1′58″N, 87°51′11″-87°51′33″W) (Fig. 1). The climate in the investigated area can best be described as humid subtropical (Reyes et al., 2018). In this area, the mean annual precipitation is 1300 mm with a mean annual temperature of 15 °C (Zhang et al., 2019). Soil in this area is formed from loess mantle over residuum from limestone. According to USDA-NRCS soil survey, the soil was categorized into Crider series and classified as fine-silty, mixed, active, mesic Typic Paleudalfs. Wheat/ double-crop soybean/ corn rotation is practiced in this field under no till soil management (Zhang et al., 2019). After planting corn, undisturbed soil cores were sampled in a 71 m by 71 m grid at 48 locations from 7 to 13 cm depth by using cutting rings (diameter: 8.4 cm, height: 6 cm, volume: 332 cm^3) in May 2017 when soil had appropriate moisture. Bulk soil samples were also collected from each location. Soil cores were used to measure hydraulic conductivity at saturated and near-saturated conditions, and bulk density. Disturbed soil samples were air-dried and passed through a 2-mm sieve for analyzing soil texture.

2.2. Laboratory analysis

The sieving and the pipette method was used to determine soil texture (Gee and Or, 2002). The volumetric cylinder method (or core method) was used to measure bulk density (ρ_b) (Grossman and Reinsch, 2002). A permeameter (Eijkelkamp, Netherlands) was used to measure saturated hydraulic conductivity based on Darcy's law under either constant or falling head condition depending on the permeability of individual soil sample (Zhang et al., 2019). A self-developed double pressure plate-membrane apparatus, which has two tension plates at the upper and lower ends of the soil sample, was used to measure near-saturated hydraulic conductivity at the matric potential of -1 cm (K_{-1}), -5 cm (K_{-5}) and -10 cm (K_{-10}) (Wendroth and Simunek, 1999). This device is similar to those used with tension infiltrometers (Zhang et al., 2019). Near-saturated hydraulic conductivity was computed based on Buckingham-Darcy's law.

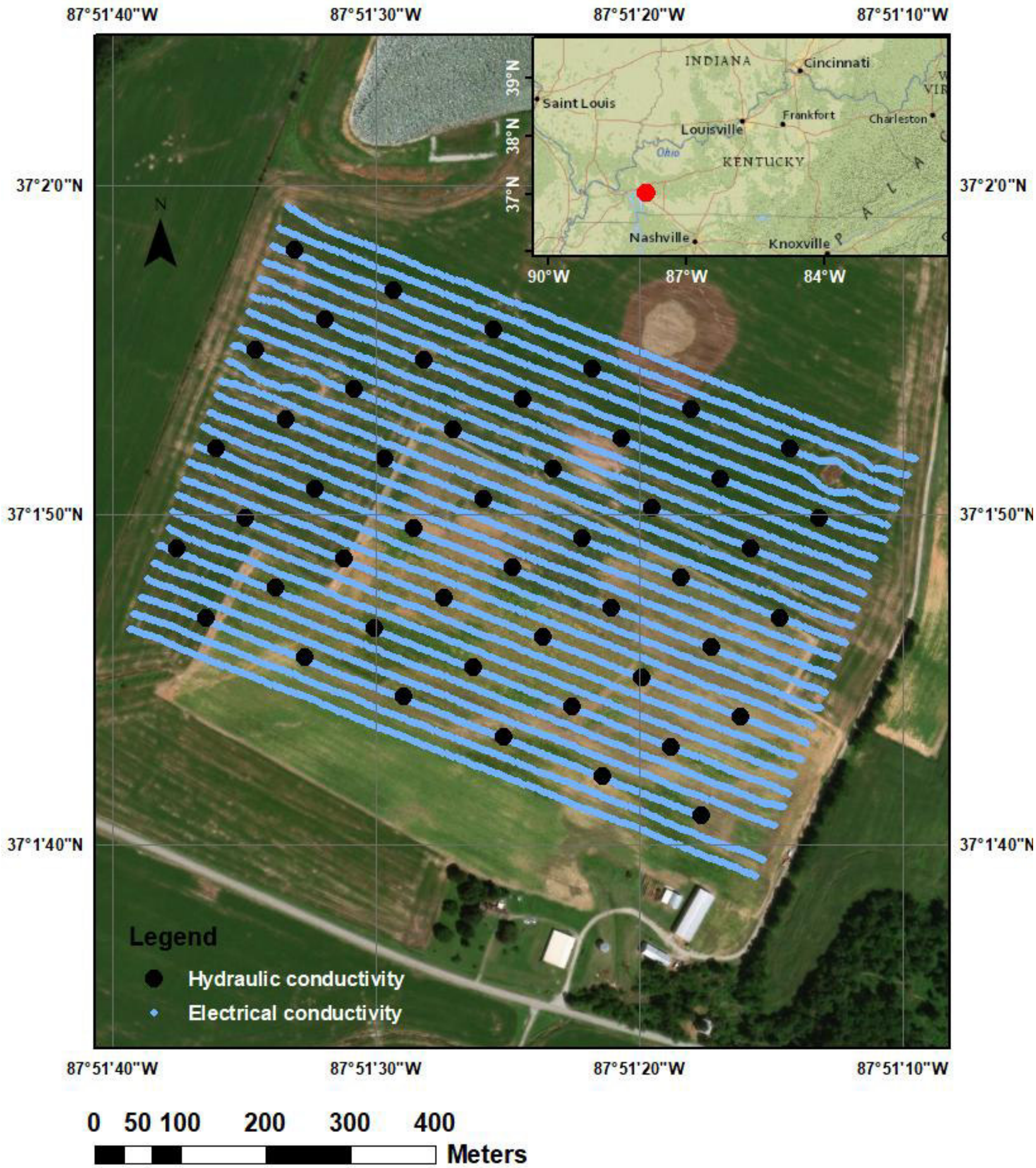

Fig. 1. Study area and sampling locations.

2.3. Estimates with pedo-transfer functions

A large number of PTFs have been developed to predict hydraulic conductivity in the past three decades. Soil texture, bulk density and organic matter were widely used as input data in these established PTFs (Wösten et al., 2001). Among these published PTFs, ROSETTA (based on 1306 soil samples in temperate to subtropical climates of North America and Europe from heterogeneous databases consisted of data from different sources and measurement procedures) and HYPRES (derived from 1139 soil samples in Europe) are the most widely used PTFs (Wösten et al., 1999; Schaap and Leij, 1998a; McBratney et al., 2011).

ROSETTA was developed based on artificial neural network analysis and includes five hierarchical models (H1 - H5) (see Schaap et al., 2001 for detail). The hierarchical structure in ROSETTA provides users with flexibility towards available input data. ROSETTA is able to estimate K_s as well as unsaturated hydraulic conductivity function parameters for the Mualem-van Genuchten model. A user-friendly computer program was developed to make the estimation with ROSETTA even more convenient. Therefore, ROSETTA was selected as an example to investigate whether PTFs reliably describe the spatial variability of hydraulic conductivity observed in a field. Based on available measured soil physical properties, the H3 model (which uses sand, silt, clay, and bulk density as input) was used to predict hydraulic conductivity in this study. Wösten (1997) emphasized that the estimation of hydraulic properties based on PTFs should be restricted to soils that fall within the range of soil textures that were used to develop the PTFs. In this study, local soil properties are within the range of the dataset that was used to develop ROSETTA.

K_s was indirectly estimated from ROSETTA. Mualem-van Genuchten model parameters were also predicted by ROSETTA using soil texture and bulk density. Using predicted K_s as a matching point combined with estimated Mualem-van Genuchten model parameters, the near-saturated hydraulic conductivity (h = -1, -5, -10 cm) was calculated by Eq. 1 (van Genuchten, 1980):

$$K(h) = K_s \frac{\{1-|\alpha h|^{n-1}[1+|\alpha h|^n]^{-m}\}^2}{[1+|\alpha h|^n]^{m/2}} \tag{1}$$

where K_s (cm day^{-1}) is the ROSETTA estimated saturated hydraulic conductivity, h (cm) is soil water pressure, α (cm^{-1}) is related to the inverse of the air-entry pressure head, m (-) and n (-) are empirical shape parameter (m=1- 1/n). α and n were predicted by ROSETTA (H3).

2.4. Geostatistical analysis

Hydraulic properties in field soils are highly variable, and any individual measurement can only provide information about the immediate vicinity of the sampled location. Information about hydraulic properties at places where no measurements are taken has to be inferred from the known values at the sampled points since only a limited number of measurements can be taken in an area (Nielsen et al., 1973; Jury and Horton, 2004). Various strategies (e.g., inverse distance weighting, kriging, cokriging) can be used to interpolate spatial data (Webster and Oliver, 2007). Geostatistics (i.e., kriging and cokriging) is generally considered as the best method for spatial interpolation and has been successfully used in studying the spatial variation of soil hydraulic properties (Vieira et al., 1981; Vauclin et al., 1983; Goovaerts, 1999; Ferrer Julià et al., 2004; Romano, 2004; Iqbal et al., 2005; Wang et al., 2013; Fu et al., 2015). Kriging is a linear interpolation that utilizes a semivariogram to estimate a variable at an unsampled location using weighted neighboring measured values (Nielsen and Wendroth, 2003). The performance of kriging in interpolating spatial data greatly depends on the quantity and quality of the measurements and their spatial continuity (Miller et al., 2007) as well as their behavior in the scale-triplet (i.e., research domain, sampling interval, and sample size) (Blöschl and Sivapalan, 1995). In a field with high spatial variability of K_s, it can be a challenge to create a set of measured K_s at a resolution that reveals a satisfactory variability structure to support kriged estimates of K_s at unsampled locations with acceptable accuracy. When K_s is undersampled, kriging is not well supported and the uncertainty of estimation poses a challenge as well. However, the estimation of K_s at unobserved locations can be improved by utilizing the relationship between K_s and easily measurable soil properties (Ersahin, 2003). Cokriging utilizes spatial information of two or more variables (one is the primary variable, the other is the ancillary variable) along with spatial cross-correlation between the two variables to estimate the undersampled variable (i.e., primary variable) at unobserved locations. The ancillary variable is spatially correlated with the variable of interest, and can be easily measured and densely sampled (Alemi et al., 1988; Nielsen and Wendroth, 2003). By using clay content (Alemi et al., 1988), bulk density (Ersahin, 2003) or water-stable aggregates (Basaran et al., 2011) as ancillary variable, cokriging has been proven to be superior to kriging in characterizing the spatial variability of K_s when K_s is only sparsely sampled in an area. Although apparent electrical conductivity has not been used as an ancillary variable in cokriging to estimate K_s, investigating the spatial association of K_s to apparent electrical conductivity might be another promising way to estimate the spatial distribution of K_s across a field. Apparent electrical conductivity (EC_a) is a simple, efficient and inexpensive measurement, and can be densely measured over large areas (Sudduth et al., 2005). Similar to water flow in soil, apparent electrical conduction (mainly through electrolyte in sufficiently moist soil) occurs in the same network of pores and channels (Corwin and Lesch, 2003; Doussan and Ruy, 2009). Apparent electrical conductivity is influenced by a variety of soil properties including soil clay content, porosity, pore connectivity, moisture, temperature, salinity, and organic matter (Corwin and Lesch, 2005; Friedman, 2005; Doussan and Ruy, 2009; Chaplot et al., 2010). These factors influencing EC_a also affect soil hydraulic conductivity. In recent studies, EC_a was successfully used as a predictor in linear regression PTFs to calculate K_s (Chaplot et al., 2011; Rezaei et al., 2016). Therefore, EC_a can be considered as an ancillary variable and was used in cokriging to facilitate the estimation of hydraulic conductivity in this research.

Soil EC_a at shallow depth (0-30 cm) was densely measured in the field (Fig. 1) (the distance between two neighboring transects was about 17 m and the distance between two neighboring points along each transect was approximately 2 m) using a Veris 3150. For details of the measurement procedure, the reader is referred to Reyes et al. (2018). Apparent electrical conductivity and hydraulic conductivity were not measured at exactly the same coordinates. In order to perform a classic cross semivariogram, the values of EC_a points (3-5 points) located within a radius of 2 m around each hydraulic conductivity sampling location were averaged and this averaged value was used as EC_a value in the point of hydraulic conductivity.

Geostatistical analysis was then conducted to characterize the spatial pattern of hydraulic conductivity and to assess the capability of ROSETTA in describing the spatial variability of hydraulic conductivity in the field. Prior to geostatistical analysis, the Kolmogorov-Smirnov (*K-S*) test (at the 5% significance level) was used to evaluate the normality of each data distribution (Bitencourt et al., 2016). The Kolmogorov-Smirnov test quantifies the maximum difference between the observed distribution function of the sample and the theoretical distribution function (Massey, 1951). All the data (hydraulic conductivity data was log-transformed) passed the *K-S* test, since the calculated maximum differences were below the critical value at the 5% significance level (Table 1). The results indicated that the dataset in this study tended to follow the normal distribution. Note that EC_a data (N = 48) at the locations of hydraulic conductivity was a subset of all EC_a measurements (N= 7416) in the studied field. Apparent electrical conductivity data including all the points failed the *K-S* test as a result of the huge number of samples considerably reduce the critical value (for α= 5%, critical value is $1.36/\sqrt{N}$). Since EC_a data (N = 48) had the same number of observations as hydraulic conductivity data and was normally distributed, EC_a data (N= 7416) distribution can still be considered as a normal distribution for practical purpose (Reyes et al., 2018).

Experimental semivariograms and cross semivariograms were calculated to describe the spatial variance structure and identify the input parameters for cokriging spatial interpolation (Nielsen and Wendroth, 2003). The experimental semivariogram and cross semivariogram were computed by Eq. 2 and Eq. 3, respectively.

$$\gamma(h) = \frac{1}{2N(h)} \sum_{i=1}^{N(h)} [Z_i(x_i) - Z_i(x_i + h)]^2 \quad (2)$$

$$\Gamma(h) = \frac{1}{2N(h)} \sum_{i=1}^{N(h)} [A_i(x_i) - A_i(x_i + h)][B_i(x_i) - B_i(x_i + h)] \quad (3)$$

where h is the separation distance or lag distance, $N(h)$ is the number of data pairs for the separation distance h, $Z_i(x_i)$ is a measured variable at spatial location x_i, $Z_i(x_i + h)$ is a measured variable at spatial location $x_i + h$, A_i and B_i indicate the primary and the ancillary variables, respectively.

Experimental semivariograms and cross semivariograms were fitted to an empirical model including an exponential component and a Gaussian component (Eq. 4) (Oliver and Webster, 2014) on top of the nugget contribution to variance.

$$\gamma(h) = C_0 + C_1\left[1 - \exp\left(-\frac{h}{a_1}\right)\right] + C_2\left[1 - \exp\left(-\frac{h^2}{a_2^2}\right)\right] \quad (4)$$

where C_0 represents the nugget effect; C_1 and C_2 are the partial sills of exponential and Gaussian components, respectively, and sill (total variation) equals to $C_0+C_1+C_2$; a_1 and a_2 are the ranges of exponential and Gaussian components, respectively; h is the lag distance. The two model functions were selected and determined principally on sum of square residuals (SSR), coefficient of determination (r^2) as well as visual fit (Cambardella et al., 1994; Wang et al., 2013).

The spatial distribution maps of hydraulic conductivity were generated using fitted semivariograms and cross semivariograms parameters through cokriging, which estimated the values of hydraulic conductivity at unobserved locations by utilizing Eq. 5.

$$A^*(x_0) = \sum_{i=1}^{p} \lambda_{Ai} A_i(x_i) + \sum_{j=1}^{q} \lambda_{Bj} B_j(x_j) \tag{5}$$

where $A^*(x_0)$ is the value of primary variable to be estimated at the location of x_0, $A_i(x_i)$ is the known value of primary variable at the sampling site x_i, $B_j(x_j)$ is the known value of ancillary variable at the sampling site x_j, λ_{Ai} and λ_{Bj} are weights ($\sum_{i=1}^{p} \lambda_{Ai} = 1$, $\sum_{j=1}^{q} \lambda_{Bj} = 0$), p and q are the number of observed sites around x_0 that are within the zone of correlation.

All the data analyses and visualization were accomplished by libraries (Gstat and Nortest) included in the R statistics environment (R Development Core Team, 2016) and ArcGIS 10.4.1.

3. Results and Discussion

3.1. Descriptive statistics of soil physical and hydraulic properties

According to USDA textural classification, three textural classes (silt loam, silt, and silty clay loam) were observed in the field (Fig. 2). Silt loam was the predominant soil texture. The bulk density ranged from 1.33 to 1.77 g cm^{-3} (Table 1). EC_a values at the points of hydraulic conductivity ranged from 2.80 to 8.40 mS m^{-1} with a mean of 4.64 mS m^{-1} (Table 1).

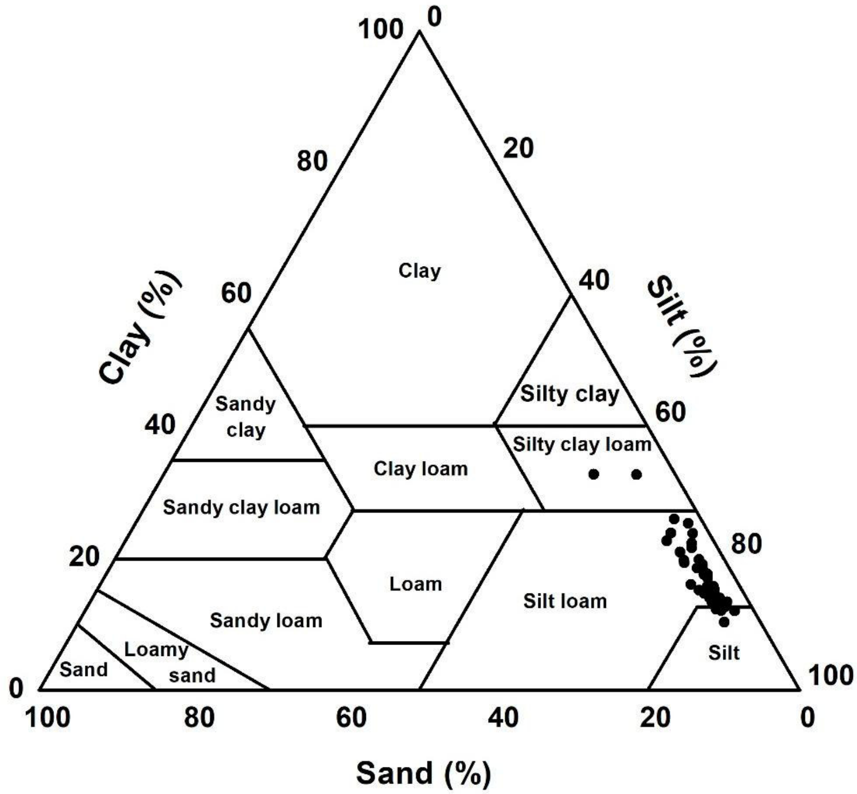

Fig. 2. Textural distribution of soils investigated in this study.

Soil hydraulic conductivity (cm day^{-1}) follows log-normal distribution. Measured hydraulic conductivity data was log-transformed. The ranges of $\log_{10} K_s$, $\log_{10} K_{-1}$, $\log_{10} K_{-5}$, and $\log_{10} K_{-10}$ were between -1.80 and 4.21, -1.15 and 2.34, -1.22 and 1.42, and -1.40 and 0.75 $\log_{10}$ (cm day^{-1}), respectively (Table 1). Note that the hydraulic conductivity near water saturation (K_{-1}, K_{-5} and K_{-10}) was slightly higher than K_s for several soil samples with low permeability. According to Vereecken et al. (2010), those slight inconsistencies might be attributed to different measurement methods. The hydraulic conductivity of soils with low permeability changed little regardless of whether the soil was measured at saturation or slight unsaturation since these samples remain fully saturated due to capillary forces even under slightly negative pressure. The measurement results obtained with different methods just reflected measurement uncertainty. The falling head method was used to determine K_s of soils with low permeability. Evaporation cannot be completely avoided during this process since the measurement took a relatively long time (Zhang et al., 2019). This might be another explanation for the underestimation of K_s.

ROSETTA-estimated hydraulic conductivity data (cm day^{-1}) was also log-transformed (Table 1). The ranges of $\log_{10} K_s$, $\log_{10} K_{-1}$, $\log_{10} K_{-5}$, and $\log_{10} K_{-10}$ were between 0.37 and 1.49, 0.26 and 1.46, 0.13 and 1.40, and 0.02 and 1.35 $\log_{10}$ (cm day^{-1}), respectively.

Table 1

Descriptive statistics for observed and ROSETTA estimated hydraulic conductivity, and basic soil physical properties over the field (N= 48).

Variables †	Maximum	Minimum	Mean	S.D. ‡	*K-S* ‡
		Observed data			
K_s, $\log_{10}$ (cm day^{-1})	4.21	-1.80	1.49	1.36	0.08
K_{-1}, $\log_{10}$ (cm day^{-1})	2.34	-1.15	0.58	0.74	0.14
K_{-5}, $\log_{10}$ (cm day^{-1})	1.42	-1.22	0.15	0.54	0.07
K_{-10}, $\log_{10}$ (cm day^{-1})	0.75	-1.40	-0.10	0.44	0.11
Sand, %	11	2	4	1	0.14
Silt, %	85	57	79	6	0.15
Clay, %	33	10	17	5	0.18
ρ_b, g cm^{-3}	1.77	1.33	1.61	0.07	0.10
EC_a, mS m^{-1}	8.40	2.80	4.64	1.23	0.09
		ROSETTA estimated data			
K_s, $\log_{10}$ (cm day^{-1})	1.49	0.37	0.87	0.22	0.12
K_{-1}, $\log_{10}$ (cm day^{-1})	1.46	0.26	0.82	0.24	0.11
K_{-5}, $\log_{10}$ (cm day^{-1})	1.40	0.13	0.73	0.25	0.12
K_{-10}, $\log_{10}$ (cm day^{-1})	1.35	0.02	0.65	0.26	0.12

† K_s, saturated hydraulic conductivity; K_{-1} K_{-5} and K_{-10}, near-saturated hydraulic conductivity at potentials of -1 cm, -5 cm and -10 cm; ρ_b, bulk density; EC_a, apparent electrical conductivity.

‡ S.D., standard deviation; *K-S*, Kolmogorov–Smirnov test for normality (for α=5%, critical value is 0.196).

The overall performance of ROSETTA (H3) in estimating hydraulic conductivity at the field scale was assessed and shown in Table 2. There was a weak relationship between measured and predicted K_s. Although the performance of ROSETTA (H3) in predicting near-saturated hydraulic conductivity was also less satisfied, it is better than the estimation of K_s.

Table 2

The performance of ROSETTA in estimating hydraulic conductivity at the field scale

Evaluation criteria†	K_s	K_{-1}	K_{-5}	K_{-10}
RMSE, $\log_{10}$ (cm day^{-1})	1.44	0.69	0.74	0.83
r^2	0.07	0.26	0.26	0.32

† RMSE (root mean square error) was calculated by $\sqrt{\frac{1}{q}\sum_{i=1}^{q}(m_i-p_i)^2}$, while r^2 (coefficient of determination) was calculated by $\left[\frac{\sum_{i=1}^{q}(m_i-\bar{m})(p_i-\bar{p})}{\sqrt{\sum_{i=1}^{q}(m_i-\bar{m})^2}\times\sqrt{\sum_{i=1}^{q}(p_i-\bar{p})^2}}\right]^2$. q is the number of observations, m_i and p_i are the i^{th} measured and predicted K (h) values, respectively, $\bar{m}$ is mean of measured K (h), and $\bar{p}$ is mean of predicted K (h).

3.2. Spatial structure of hydraulic conductivity

Semivariograms and cross semivariograms based on measured and ROSETTA-estimated data are shown in Figures 3 and 4. A nested model including an exponential and a Gaussian component was used to fit the experimental semivariograms and cross semivariograms. Theoretically, semivariance increases with lag distance to a plateau or constant value (total semivariance) at a given separation distance (the range of spatial dependence) (Trangmar et al., 1986). Samples separated by distances less than the range are spatially correlated, while those separated by distances beyond the range are not spatially correlated (Wang et al., 2013). The range indicates the maximum distance over which neighboring observations are spatially related. Beyond the range, lag distances should be disregarded for interpolation (Nielsen and Wendroth, 2003). The shorter the range, the more heterogeneous the variable is; while the longer the range, the more homogeneous or spatially continuous the variable behaves (Marín-Castro et al., 2016). The non-zero semivariance at lag distance of zero is called nugget semivariance (C_0), which represents measurement errors or microvariability of the variable occurring over smaller distance than the sampling interval (Trangmar et al., 1986; Nielsen and Wendroth, 2003). The ratio between nugget and total semivariance (or relative nugget effect, RNE), $C_0/(C_0+C_1+C_2)$, was used to evaluate the strength of spatial dependence with the sampling interval taken: strong if the ratio was less than 25%, moderate if the ratio was between 25% and 75%, and weak if the ratio was greater than 75% (Cambardella et al., 1994).

The measured K_s was weakly spatially dependent (RNE= 81%), while measured near-saturated hydraulic conductivity was moderately spatially dependent with the relative nugget effect ranging from about 46% to 48% (Fig. 3 a-d). K_s revealed a high relative nugget effect, which means short range effects (or microheterogeneity) of K_s in the field cannot be detected at the scale of sampling (Trangmar et al., 1986). K_s might exhibit stronger spatial dependence at a scale smaller than the sampling interval. In Fig. 3 b-d, note that the range values for near-saturated hydraulic conductivity were significantly larger than the range for K_s. For instance, K_s had a range value of 209 m, while the range values for near-saturated hydraulic conductivity (K_{-1}, K_{-5} and K_{-10}) were 389 m, 418 m, and 474 m, respectively. This result indicated that the spatial distribution of K_s was more heterogeneous than the spatial distribution of near-saturated hydraulic conductivity. The high heterogeneity of K_s might be caused by potential macropore effects. At saturation, all pores conduct water and macropores greatly contribute to water flow. The presence of one single macropore is barely manifested in the total porosity, however, can greatly contribute to K_s if the pore is continuous and connected to other pores. As the matric potential decreases, the water-transmitting pores are those with smaller diameters (meso- and micro-pores). Since macropores are determined by soil structure, which is significantly influenced by external disturbance, their variation would be larger than that of smaller pores inherent in the soil matrix (Mohanty et al., 1994). The inherent relationship between K_s and macropores is therefore critical for the spatial structure of K_s at the field scale (Marín-Castro et al., 2016).

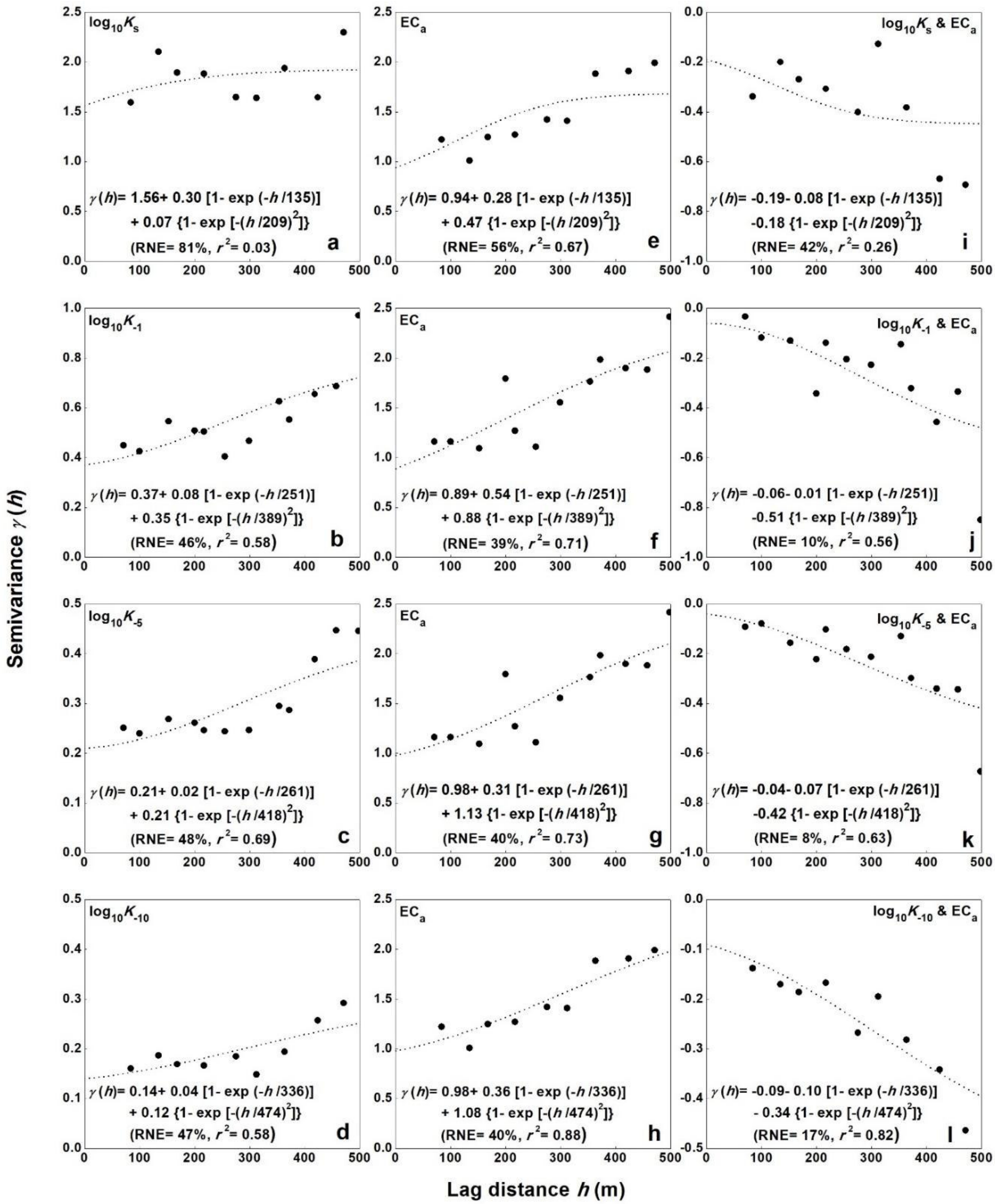

Fig. 3. Semivariograms for measured hydraulic conductivity and apparent electrical conductivity (EC_a). (a-d: semivariograms of measured hydraulic conductivity, e-h: semivariograms of EC_a, i-l: cross semivariograms of measured hydraulic conductivity and EC_a)

Note: K_s is saturated hydraulic condcutivity, while K_{-1}, K_{-5} and K_{-10} are near-saturated hydraulic conductivity at matric potentials of -1 cm, -5 cm and -10 cm.

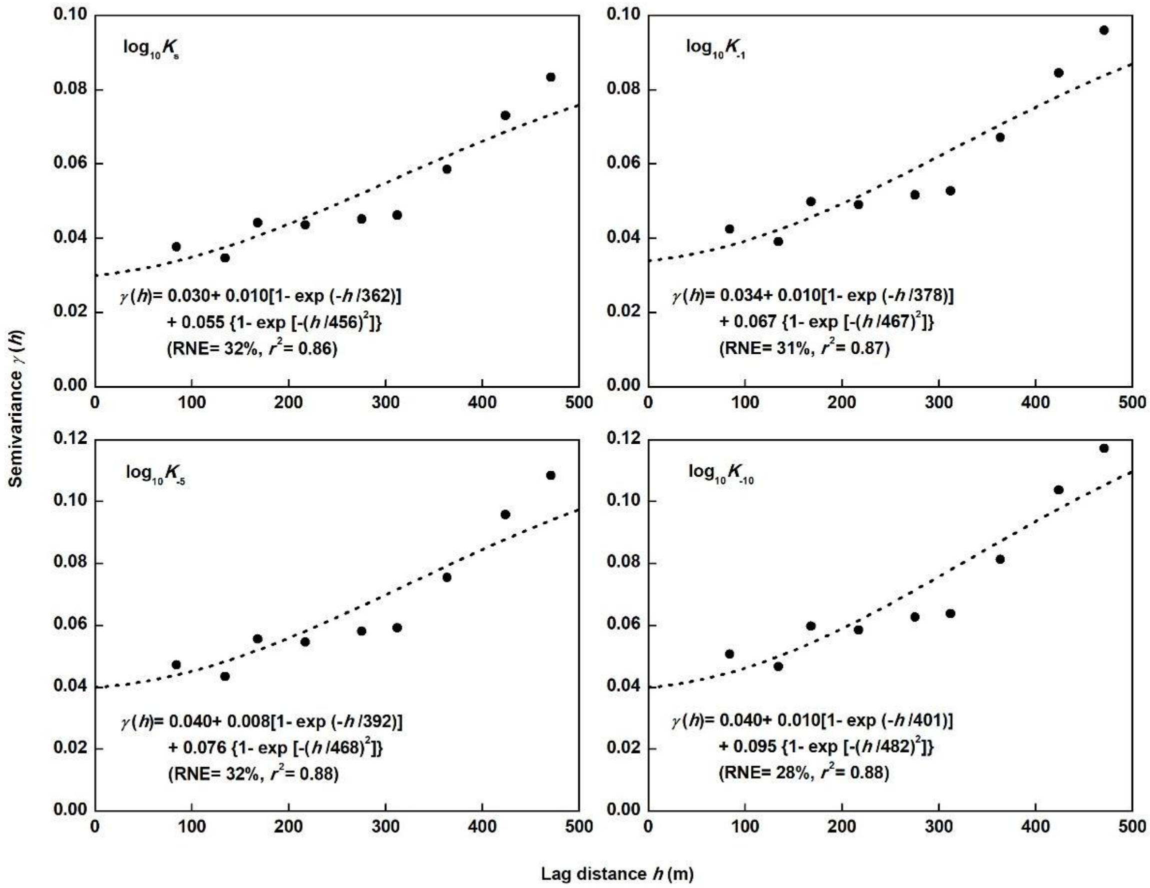

Fig. 4. Semivariograms for estimated hydraulic conductivity with ROSETTA

Note: K_s is saturated hydraulic condcutivity, while K_{-1}, K_{-5} and K_{-10} are near-saturated hydraulic conductivity at matric potentials of -1 cm, -5 cm and -10 cm.

For the ROSETTA estimated hydraulic conductivity under saturated and near-saturated conditions, the corresponding relative nugget effect ranged from 28% to 32% (Fig. 4). Therefore, ROSETTA estimated hydraulic conductivity showed a moderate spatial dependence that is more pronounced than that of the measured hydraulic conductivity, especially for K_s, which had an RNE of 81%. Semivariances for hydraulic conductivity predicted by ROSETTA (Fig. 4) were consistently smaller than those for measured hydraulic conductivity (Fig. 3 a-d). Also, the range values for ROSETTA-predicted data were larger than those for measured data. For example, predicted K_s had a range value of 456 m, while the range values for measured K_s was only 209 m. These results indicated that ROSETTA-estimated hydraulic conductivity was more homogeneous or continuous than measured data in the field. This phenomenon might be a result of the estimates being calculated mainly based on soil texture-related properties. The spatial structure of ROSETTA-estimated hydraulic conductivity followed the spatial structure of clay content in the same field (Reyes et al., 2018). The spatial variability exhibited by ROSETTA estimates was therefore dominated by textural properties, which represented the intrinsic variation (e.g., texture, mineralogy) inherited from soil genesis. However, the field in this study has a narrow range of soil texture and bulk density. Moreover, at the field scale, wet-range hydraulic conductivity is rather sensitive to soil structure, which has high variation and is strongly influenced by extrinsic variations (e.g., biological activity, agricultural management) (Jarvis et al., 2002). Therefore, the variability of saturated and near-saturated hydraulic conductivity in the field cannot be reflected by the variation in texture and bulk density (Zhang et al., 2019). Both intrinsic and extrinsic factors (sometimes the internal factors can be masked by the external factors) dominated the semivariograms based on measurements, whereas only intrinsic factors influenced the semivariograms of PTF estimates and the following interpolated maps. Compared with intrinsic factors, extrinsic factors show much more spatial heterogeneity (Cambardella et al., 1994; Romano, 2004). Therefore, measured hydraulic conductivity exhibited more heterogeneity and weaker spatial dependence than ROSETTA estimates.

Based on measured data, there was a good spatial correlation (RNE ranged from about 8% to 42%) between hydraulic conductivity and apparent electrical conductivity (Fig. 3 i-l). This spatial relationship was represented by a rapidly decreasing cross semivariance calculated between hydraulic conductivity and EC_a values, which indicated that high values of hydraulic conductivity corresponded to low values of EC_a, and vice versa. This result suggested that EC_a could be used as an ancillary variable to predict the spatial distribution of saturated and near-saturated hydraulic conductivity with co-regionalization analysis in the field. This approach would be preferred, as EC_a can be easily and accurately determined.

3.3. Spatial distribution of hydraulic conductivity

The fitted semivariogram and cross semivariogram models for measured hydraulic conductivity were used in cokriging to generate hydraulic conductivity maps with a resolution of 2×2 m^2. Based on measured data, K_s (Fig. 5 a) showed very strong spatial variability and was markedly different from the spatial patterns of near-saturated hydraulic conductivity (Fig. 5 b-d). As soil water pressure approached zero, hydraulic conductivity may depend to a large extent on small number of large pores (Bodhinayake and Si, 2004). Soil pores with equivalent diameters larger than 300 μm (i.e., soil water pressure of -10 cm) have profound influence on water movement in a field with well-structured soils (Jarvis et al., 2002; Jarvis, 2007). Hydraulic conductivity close to saturation ($h \geq$ -10 cm) is therefore important to illustrate macropore effects.

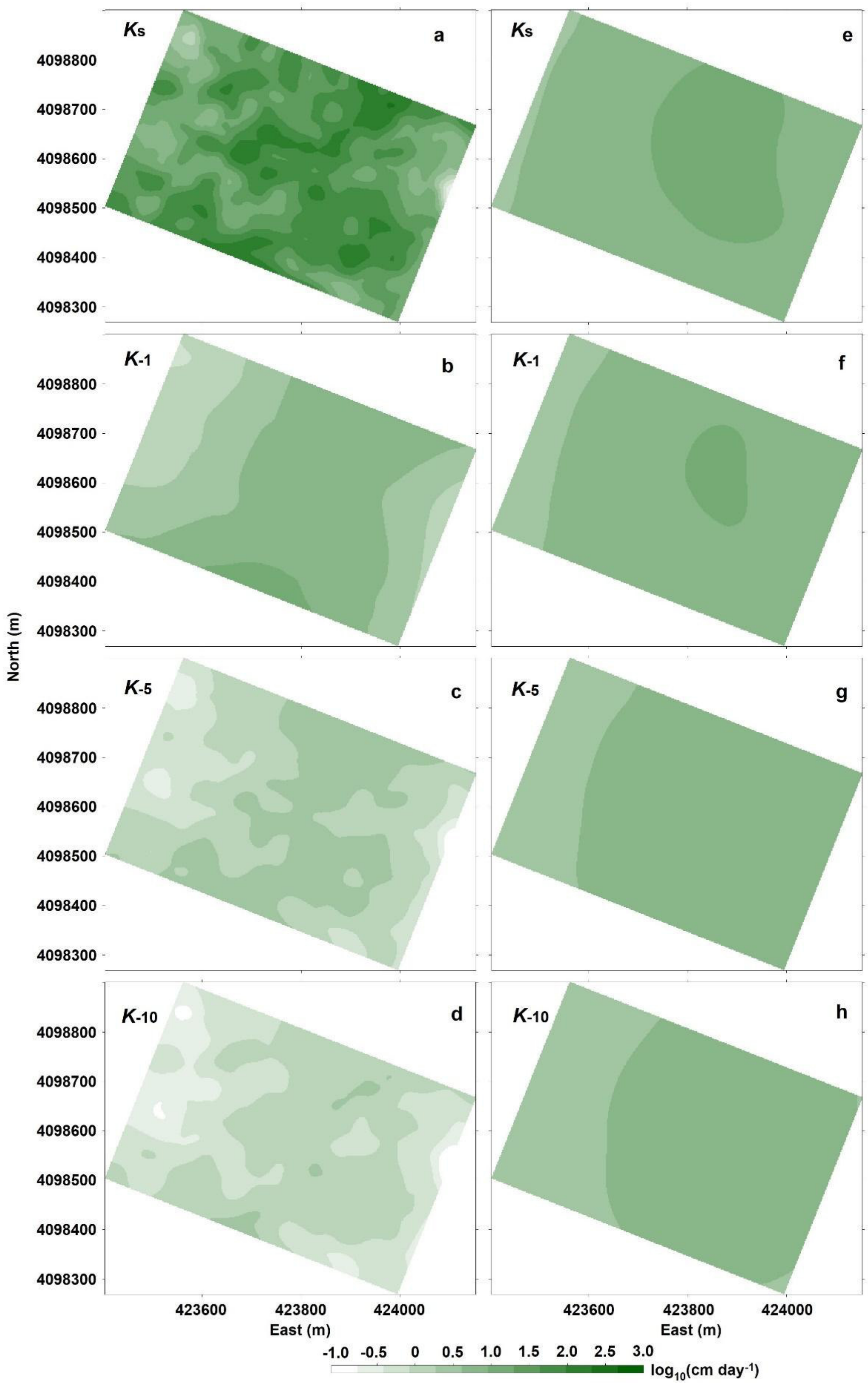

Fig. 5. Spatial patterns of hydraulic conductivity based on measured data (a-d) and predicted data from ROSETTA (e-h).

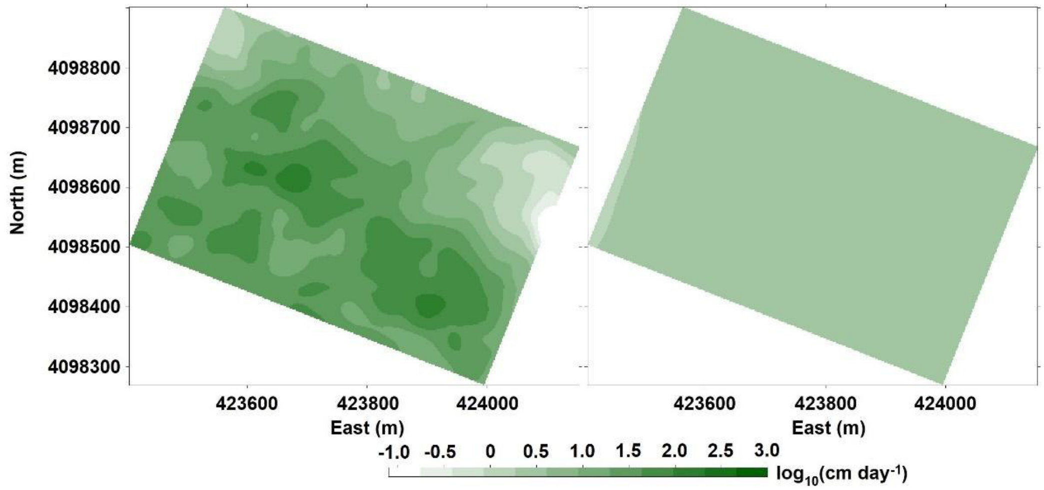

Fig. 6. Spatial patterns of macropore hydraulic conductivity based on measured data (left) and predicted data from ROSETTA (right).

A significant reduction in hydraulic conductivity near saturation can be detected in soil with structural macropores when these pores drain under slight pressure and do not contribute to flow anymore (Jarvis et al., 2002). Macropore hydraulic conductivity can be defined as the difference between K_s and K_{-10} (i.e., K_s - K_{-10}) (Jarvis et al., 2013). By comparing measured hydraulic conductivity maps, a large reduction (~95%) in hydraulic conductivity was observed in the field when soil water pressure head decreased from 0 to -10 cm. The decrease in hydraulic conductivity was due to emptying of continuous macropores. The spatial pattern of macropore hydraulic conductivity (K_s - K_{-10}) in the field was further characterized and was shown in Fig. 6. The macropore hydraulic conductivity calculated from measured data also exhibited high heterogeneity in the field (left in Fig. 6). Note that the K_s map (Fig. 5a) and macropore hydraulic conductivity map generated from measured data (left in Fig. 6) showed similarity for major areas in the field. This result indicated that macropore effects were predominant in the studied field and had a great contribution to K_s. The presence of large pores increased the spatial variability of K_s in the field.

The spatial patterns of hydraulic conductivity in the same field were also generated with ROSETTA-predicted data (Fig. 5 e-h). The ROSETTA-estimated K_s map behaved similar to the corresponding spatial distributions of near-saturated hydraulic conductivity. Compared with measured data, the K_s map obtained using PTF-estimated data showed less heterogeneity. Also, the macropore hydraulic conductivity calculated based on PTFs estimates was much more homogeneous in the field and had relatively small magnitude (right in Fig. 6). This result indicated that ROSETTA is incapable of identifying the macropore effects observed in the field. Structural macropores are particularly important in the wet range of hydraulic conductivity function (Weynants et al., 2009). Soil pore space is influenced by particle-size distribution, however, it cannot be estimated solely from soil texture (Lin et al., 1999a). Although bulk density, which is an indicator of soil porosity, is included in ROSETTA, it is hardly related to hydraulic conductivity close to saturation (Zhang et al., 2019). Few macropores have very little contribution to total porosity and therefore bulk density, however, they can cause rapid water flow in aggregated or no-till soil with a hierarchical pore organization (Beven and Germann, 1982). Unfortunately, soil structural macropore information is rarely incorporated in established PTFs, since this information is unavailable in most databases. Therefore, the variance of K_s observed in this field was significantly underestimated by ROSETTA, which is a texture-dominated PTF. Although pseudosand (the cementing action of iron oxides and other inorganic compounds produces very stable small aggregates in some highly weathered clayey soils, such as Ultisols and Oxisols) is less common in Alfisols (Weil and Brady, 2016), it might be another explanation for the discrepancies between measured and PTF-estimated K_s. Soil hydraulic conductivity can be influenced by these small aggregates, which were destroyed by chemical treatments during sieving and the pipette method. However, most PTFs (e.g., ROSETTA) were based on soil textural information that was determined according to this standard lab protocols (Wösten et al., 2001). It would certainly be important to derive a dataset that is based on "effective" particle size and then derive relationships between this effective particle size composition and hydraulic properties.

Based on measured hydraulic conductivity, near-saturated hydraulic conductivity exhibited a spatially more homogeneous pattern than measured K_s (Fig. 5 b-d). Note that although ROSETTA slightly overestimated the values, the spatial patterns of measured hydraulic conductivity in major areas can still be captured by estimated data when the matric potential decreased to -10 cm (Fig. 5 d and h). This result suggested that established PTFs, in which soil structure or macropore effects are not taken into account, might be still suitable for studying the spatial variability of unsaturated hydraulic conductivity that is not strongly influenced by soil structure as K_s, but will lack precision when used for characterizing spatial distribution of K_s in a field with structural soils. This result is consistent with the observations reported by da Silva et al. (2017), who found that the observed spatial pattern of unsaturated hydraulic conductivity can be reasonably predicted by ROSETTA-estimated data. The findings also indicated that hydraulic conductivity measured at saturation, which is sensitive to macropore effects, might not be an appropriate matching point for unsaturated hydraulic conductivity function. The unsaturated flow, which occurs in the soil matrix, might be overestimated by using measured K_s as matching point for hydraulic conductivity function (Schaap and Leij, 2000; Jarvis et al., 2002). Hydraulic conductivity measured at slightly unsaturated condition (Ehlers, 1977) or PTFs-estimated K_s might be a better alternative to be used as a matching point.

4. Conclusions

In this study, the spatial variability of wet range hydraulic conductivity observed in a no-till farmland was characterized with co-regionalization analysis and compared with the spatial variability of the results simulated with the ROSETTA PTF. In the studied field, measured saturated hydraulic conductivity showed high spatial heterogeneity because of macropore effects. The strong spatial variation in saturated hydraulic conductivity was not captured by PTF estimates since soil structure information is not included, although ROSETTA could reasonably generate the relative spatial pattern of unsaturated hydraulic conductivity. The K_s map based on PTF estimates should be evaluated carefully and handled with caution, especially when the map is used for precision resources management. This study also indicated that saturated hydraulic conductivity should be measured at closer intervals to obtain more spatial information and improve the performance of spatial interpolation.

Acknowledgements

The authors thank Riley Jason Walton for his excellent technical support and the farmer Trevor Gilkey for allowing us to conduct this research in his field (Hillview Farms). The authors thank Diane Hunter, Division of Regulatory Services, University of Kentucky, for her help in soil analysis. We gratefully acknowledge the support of this project by United States Geological Survey and Kentucky Water Resources Research Institute 104-B Student Research Enhancement Program. Support from the Water Quality Program SB 271 at the College of Agriculture, Food and Environment at the University of Kentucky is appreciated. This work is supported by the USDA National Institute of Food and Agriculture, Multistate Project KY006093.

References

Al-Karadsheh, E., Sourell, H., Krause, R., 2002. Precision irrigation: new strategy irrigation water management. In: Proc. Conference on International Agricultural Research for Development. Deutscher Tropentag, Witzenhausen, October 9-11.

Alemi, M.H., Shahriari, M.R., Nielsen, D.R., 1988. Kriging and cokriging of soil water properties. Soil Technol. 1, 117-132.

Alvarez-Acosta, C., Lascano, R.J., Stroosnijder, L., 2012. Test of the ROSETTA pedotransfer function for saturated hydraulic conductivity. Open J. Soil Sci. 2, 203 - 212.

Amoozegar, A., 1989. A compact constant-head permeameter for measuring saturated hydraulic conductivity of the vadose zone. Soil Sci. Soc. Am. J. 53, 1356-1361.

Basaran, M., Erpul, G., Ozcan, A.U., Saygin, D.S., Kibar, M., Bayramin, I., Yilman, F.E., 2011. Spatial information of soil hydraulic conductivity and performance of cokriging over kriging in a semi-arid basin scale. Environ. Earth Sci. 63, 827-838.

Berli, M., Carminati, A., Ghezzehei, T. A., Or, D., 2008. Evolution of unsaturated hydraulic conductivity of aggregated soils due to compressive forces. Water Resour. Res. 44, W00C09.

Beven, K., Germann, P., 1982. Macropores and water flow in soils. Water Resour. Res. 18:1311-1325.

Bitencourt, D.G.B., Barros, W.S., Timm, L.C., She, D., Penning, L.H., Parfitt, J.M.B., Reichardt, K., 2016. Multivariate and geostatistical analyses to evaluate lowland soil levelling effects on physico-chemical properties. Soil Till. Res. 156, 63-73.

Blöschl, G., Sivapalan, M., 1995. Scale issues in hydrological modelling: a review. Hydrol. Process. 9, 251-290.

Bodhinayake, W., Si, B.C., 2004. Near-saturated surface soil hydraulic properties under different land uses in the St Denis National Wildlife Area, Saskatchewan, Canada. Hydrol. Process. 18, 2835-2850.

Bouma, J., Jongerius, A., Boersma, O., Jager, A., Schoonderbeek, D., 1977. The function of different types of macropores during saturated flow through four swelling soil horizons. Soil Sci. Soc. Am. J. 41, 945-950.

Braud, I., Desprats, J.F., Ayral, P.A., Bouvier, C., Vandervaere, J.P., 2017. Mapping topsoil field-saturated hydraulic conductivity from point measurements using different methods. J. Hydrol. Hydromech. 65, 264-275.

Buttle, J.M., House, D.A., 1997. Spatial variability of saturated hydraulic conductivity in shallow macroporous soils in a forested basin. J. Hydrol. 203, 127-142.

Cambardella, C.A., Moorman, T.B., Parkin, T.B., Karlen, D.L., Novak, J.M., Turco, R.F., Konopka, A.E., 1994. Field-scale variability of soil properties in central Iowa soils. Soil Sci. Soc. Am. J. 58, 1501-1511.

Chaplot, V., Jewitt, G., Lorentz, S., 2011. Predicting plot-scale water infiltration using the correlation between soil apparent electrical resistivity and various soil properties. Phys. Chem. Earth Pts A/B/C 36, 1033-1042.

Chaplot, V., Lorentz, S., Podwojewski, P., Jewitt, G., 2010. Digital mapping of A-horizon thickness using the correlation between various soil properties and soil apparent electrical resistivity. Geoderma 157, 154-164.

Chirico, G.B., Medina, H., Romano, N., 2007. Uncertainty in predicting soil hydraulic properties at the hillslope scale with indirect methods. J. Hydrol. 334, 405-422.

Corwin, D.L., Lesch, S.M., 2003. Application of soil electrical conductivity to precision agriculture. Agron. J. 95, 455-471.

Corwin, D.L., Lesch, S.M., 2005. Characterizing soil spatial variability with apparent soil electrical conductivity: I. Survey protocols. Comput. Electron. Agr. 46, 103-133.

da Silva, A.C., Armindo, R.A., Brito, A.d.S., Schaap, M.G., 2017. An assessment of pedotransfer function performance for the estimation of spatial variability of key soil hydraulic properties. Vadose Zone J. 16.

Doussan, C., Ruy, S., 2009. Prediction of unsaturated soil hydraulic conductivity with electrical conductivity. Water Resour. Res. 45, W10408.

Ehlers, W., 1977. Measurement and calculation of hydraulic conductivity in horizons of tilled and untilled loess-derived soil, Germany. Geoderma 19, 293-306.

Ersahin, S., 2003. Comparing ordinary kriging and cokriging to estimate infiltration rate. Soil Sci. Soc. Am. J. 67, 1848-1855.

Ferrer Julià, M., Estrela Monreal, T., Sánchez del Corral Jiménez, A., García Meléndez, E., 2004. Constructing a saturated hydraulic conductivity map of Spain using pedotransfer functions and spatial prediction. Geoderma 123, 257-277.

Friedman, S.P., 2005. Soil properties influencing apparent electrical conductivity: a review. Comput. Electron. Agr. 46, 45-70.

Fu, T., Chen, H., Zhang, W., Nie, Y., Wang, K., 2015. Vertical distribution of soil saturated hydraulic conductivity and its influencing factors in a small karst catchment in Southwest China. Environ. Monit. Assess. 187, 92-94.

Gadi, V.K., Tang, Y.R., Das, A., Monga, C., Garg, A., Berretta, C., Sahoo, L., 2017. Spatial and temporal variation of hydraulic conductivity and vegetation growth in green infrastructures using infiltrometer and visual technique. CATENA 155, 20-29.

Gee, G.W., Or, D., 2002. Particle-size analysis. in: Dane, J.H., Topp, C.G. (Eds.), Methods of Soil Analysis: Part 4 Physical Methods. Soil Science Society of America, Madison, WI, pp. 255-293.

Germán Soracco, C., Lozano, L.A., Sarli, G.O., Gelati, P.R., Filgueira, R.R., 2010. Anisotropy of saturated hydraulic conductivity in a soil under conservation and no-till treatments. Soil Till. Res. 109, 18-22.

Goovaerts, P., 1999. Geostatistics in soil science: state-of-the-art and perspectives. Geoderma 89, 1-45.

Grossman, R.B., Reinsch, T.G., 2002. Bulk density and linear extensibility. in: Dane, J.H., Topp, C.G. (Eds.), Methods of Soil Analysis: Part 4 Physical Methods. Soil Science Society of America, Madison, WI, pp. 201-228.

Gumiere, S.J., Lafond, J.A., Hallema, D.W., Périard, Y., Caron, J., Gallichand, J., 2014. Mapping soil hydraulic conductivity and matric potential for water management of cranberry: characterisation and spatial interpolation methods. Biosyst. Eng. 128, 29-40.

Iqbal, J., Thomasson, J.A., Jenkins, J.N., Owens, P.R., Whisler, F.D., 2005. Spatial variability analysis of soil physical properties of alluvial soils. Soil Sci. Soc. Am. J. 69, 1338-1350.

Jarvis, N., Koestel, J., Messing, I., Moeys, J., Lindahl, A., 2013. Influence of soil, land use and climatic factors on the hydraulic conductivity of soil. Hydrol. Earth Syst. Sci. 17, 5185-5195.

Jarvis, N.J., 2007. A review of non-equilibrium water flow and solute transport in soil macropores: principles, controlling factors and consequences for water quality. Eur. J. Soil Sci. 58, 523-546.

Jarvis, N.J., Messing, I., 1995. Near-saturated hydraulic conductivity in soils of contrasting texture measured by tension infiltrometers. Soil Sci. Soc. Am. J. 59, 27-34.

Jarvis, N.J., Zavattaro, L., Rajkai, K., Reynolds, W.D., Olsen, P.A., McGechan, M., Mecke, M., Mohanty, B., Leeds-Harrison, P.B., Jacques, D., 2002. Indirect estimation of near-saturated hydraulic conductivity from readily available soil information. Geoderma 108, 1-17.

Jury, W.A., Horton, R., 2004. Soil Physics. 6th ed. John Wiley & Sons Inc., Hoboken, New Jersey.

Klute, A., Dirksen, C., 1986. Hydraulic conductivity and diffusivity: laboratory methods. in: Klute, A. (Ed.), Methods of Soil Analysis: Part 1-Physical and Mineralogical Methods. Soil Science Society of America, American Society of Agronomy, Madison, WI, pp. 687-734.

Leij, F.J., Romano, N., Palladino, M., Schaap, M.G., Coppola, A., 2004. Topographical attributes to predict soil hydraulic properties along a hillslope transect. Water Resour. Res. 40, W02407.

Li, Y., Chen, D., White, R.E., Zhu, A., Zhang, J., 2007. Estimating soil hydraulic properties of Fengqiu County soils in the North China Plain using pedo-transfer functions. Geoderma 138, 261-271.

Liao, K.H., Xu, S.H., Wu, J.C., Ji, S.H., Lin, Q., 2011. Assessing soil water retention characteristics and their spatial variability using pedotransfer functions. Pedosphere 21, 413-422.

Lin, H.S., McInnes, K.J., Wilding, L.P., Hallmark, C.T., 1999a. Effects of soil morphology on hydraulic properties I. Quantification of soil morphology. Soil Sci. Soc. Am. J. 63, 948-954.

Lin, H.S., McInnes, K.J., Wilding, L.P., Hallmark, C.T., 1999b. Effects of soil morphology on hydraulic properties II. Hydraulic pedotransfer functions. Soil Sci. Soc. Am. J. 63, 955-961.

Mallants, D., Mohanty, B.P., Vervoort, A., Feyen, J., 1997. Spatial analysis of saturated hydraulic conductivity in a soil with macropores. Soil Technol. 10, 115-131.

Marín-Castro, B.E., Geissert, D., Negrete-Yankelevich, S., Gómez-Tagle Chávez, A., 2016. Spatial distribution of hydraulic conductivity in soils of secondary tropical montane cloud forests and shade coffee agroecosystems. Geoderma 283, 57-67.

Massey, F.J., 1951. The Kolmogorov-Smirnov test for goodness of fit. J. Am. Stat. Assoc. 46, 68-78.

McBratney, A.B., Minasny, B., Tranter, G., 2011. Necessary meta-data for pedotransfer functions. Geoderma 160, 627-629.

Miller, J., Franklin, J., Aspinall, R., 2007. Incorporating spatial dependence in predictive vegetation models. Ecol. Model. 202, 225-242.

Mohanty, B.P., Ankeny, M.D., Horton, R., Kanwar, R.S., 1994. Spatial analysis of hydraulic conductivity measured using disc infiltrometers. Water Resour. Res. 30, 2489-2498.

Nielsen, D., Biggar, J., Erh, K., 1973. Spatial variability of field-measured soil-water properties. Hilgardia 42, 215-259.

Nielsen, D.R., Wendroth, O., 2003. Spatial and Temporal Statistics: Sampling Field Soils and Their Vegetation. Catena Verlag, Reiskirchen, Germany.

Oliver, M.A., Webster, R., 2014. A tutorial guide to geostatistics: computing and modelling variograms and kriging. CATENA 113, 56-69.

Pringle, M.J., Romano, N., Minasny, B., Chirico, G.B., Lark, R.M., 2007. Spatial evaluation of pedotransfer functions using wavelet analysis. J. Hydrol. 333, 182-198.

Reyes, J., Wendroth, O., Matocha, C.J., Zhu, J., Ren, W., Karathanasis, A.D., 2018. Reliably mapping clay content coregionalized with electrical conductivity. Soil Sci. Soc. Am. J. 82, 578-592.

Rezaei, M., Saey, T., Seuntjens, P., Joris, I., Boënne, W., van Meirvenne, M., Cornelis, W., 2016. Predicting saturated hydraulic conductivity in a sandy grassland using proximally sensed apparent electrical conductivity. J. Appl. Geophys. 126, 35-41.

Rienzner, M., Gandolfi, C., 2014. Investigation of spatial and temporal variability of saturated soil hydraulic conductivity at the field-scale. Soil Till. Res. 135, 28-40.

Romano, N., 2004. Spatial structure of PTF estimates. Dev. Soil Sci. 30, 295-319.

Schaap, M.G., Leij, F.J., 1998a. Database-related accuracy and uncertainty of pedotransfer functions. Soil Sci. 163, 765-779.

Schaap, M.G., Leij, F.J., 1998b. Using neural networks to predict soil water retention and soil hydraulic conductivity. Soil Till. Res. 47, 37-42.

Schaap, M.G., Leij, F.J., 2000. Improved prediction of unsaturated hydraulic conductivity with the Mualem-van Genuchten model. Soil Sci. Soc. Am. J. 64, 843-851.

Schaap, M.G., Leij, F.J., van Genuchten, M.T., 2001. ROSETTA: a computer program for estimating soil hydraulic parameters with hierarchical pedotransfer functions. J. Hydrol. 251, 163-176.

Springer, E.P., Cundy, T.W., 1987. Field-scale evaluation of infiltration parameters from soil texture for hydrologic analysis. Water Resour. Res. 23, 325-334.

Stephens, D.B., 1992. Application of the borehole permeameter. in: Topp, G.C., Reynolds, W.D., Green, R.E. (Eds.), Advances in Measurement of Soil Physical Properties: Bringing Theory into Practice. Soil Science Society of America, Madison, WI, pp. 43-68.

Strudley, M.W., Green, T.R., Ascough Ii, J.C., 2008. Tillage effects on soil hydraulic properties in space and time: state of the science. Soil Till. Res. 99, 4-48.

Sudduth, K.A., Kitchen, N.R., Wiebold, W.J., Batchelor, W.D., Bollero, G.A., Bullock, D.G., Clay, D.E., Palm, H.L., Pierce, F.J., Schuler, R.T., Thelen, K.D., 2005. Relating apparent electrical conductivity to soil properties across the north-central USA. Comput. Electron. Agr. 46, 263-283.

Tietje, O., Hennings, V., 1996. Accuracy of the saturated hydraulic conductivity prediction by pedo-transfer functions compared to the variability within FAO textural classes. Geoderma 69, 71-84.

Trangmar, B.B., Yost, R.S., Uehara, G., 1986. Application of geostatistics to spatial studies of soil properties. Adv. Agron. 38, 45-94.

Ugarte Nano, C.C., Nicolardot, B., Ubertosi, M., 2015. Near-saturated hydraulic conductivity measured on a swelling silty clay loam for three integrated weed management based cropping systems. Soil Till. Res. 150, 192-200.

van Genuchten, M.T., 1980. A closed-form equation for predicting the hydraulic conductivity of unsaturated soils. Soil Sci. Soc. Am. J. 44, 892-898.

Vauclin, M., Vieira, S.R., Vachaud, G., Nielsen, D.R., 1983. The use of cokriging with limited field soil observations. Soil Sci. Soc. Am. J. 47, 175-184.

Vereecken, H., Weynants, M., Javaux, M., Pachepsky, Y., Schaap, M.G., van Genuchten, M.T., 2010. Using pedotransfer functions to estimate the van Genuchten-Mualem soil hydraulic properties: a review. Vadose Zone J. 9, 795-820.

Vieira, S.R., Nielsen, D.R., Biggar, J.W., 1981. Spatial variability of field-measured infiltration rate. Soil Sci. Soc. Am. J. 45, 1040-1048.

Wagner, B., Tarnawski, V.R., Hennings, V., Müller, U., Wessolek, G., Plagge, R., 2001. Evaluation of pedo-transfer functions for unsaturated soil hydraulic conductivity using an independent data set. Geoderma 102, 275-297.

Wang, Y., Shao, M.A., Liu, Z., 2012. Pedotransfer functions for predicting soil hydraulic properties of the Chinese Loess Plateau. Soil Sci. 177, 424-432.

Wang, Y., Shao, M.A., Liu, Z., Horton, R., 2013. Regional-scale variation and distribution patterns of soil saturated hydraulic conductivities in surface and subsurface layers in the loessial soils of China. J. Hydrol. 487, 13-23.

Webster, R., Oliver, M.A., 2007. Geostatistics for Environmental Scientists. 2nd ed. John Wiley & Sons Ltd., Chichester, England.

Weil, R.R., Brady, N.C., 2016. The Nature and Property of Soils. 15th ed. Pearson, Upper Saddle River, NJ.

Wendroth, O., Simunek, J., 1999. Soil hydraulic properties determined from evaporation and tension infiltration experiments and their use for modeling field moisture status. In: van Genuchten, M.T., Leij, F.J., Wu, L. (Eds), Proceedings of the international workshop on characterization and measurement of the hydraulic properties of unsaturated porous media. Held in Riverside, CA, October 22-24, 1997. U.S. Salinity Laboratory, Riverside, CA. pp. 737-748.

Weynants, M., Vereecken, H., Javaux, M., 2009. Revisiting Vereecken pedotransfer functions: introducing a closed-form hydraulic model. Vadose Zone J. 8, 86-95.

Wösten, J.H.M., 1997. Pedotransfer functions to evaluate soil quality. Dev. Soil Sci. 25, 221-245.

Wösten, J.H.M., Lilly, A., Nemes, A., Le Bas, C., 1999. Development and use of a database of hydraulic properties of European soils. Geoderma 90, 169-185.

Wösten, J.H.M., Pachepsky, Y.A., Rawls, W.J., 2001. Pedotransfer functions: bridging the gap between available basic soil data and missing soil hydraulic characteristics. J. Hydrol. 251, 123-150.

Yao, R.J., Yang, J.S., Wu, D.H., Li, F.R., Gao, P., Wang, X.P., 2015. Evaluation of pedotransfer functions for estimating saturated hydraulic conductivity in coastal salt-affected mud farmland. J. Soils Sediments 15, 902-916.

Zhang, X., Zhu, J., Wendroth, O., Matocha, C., Edwards, D., 2019. Effect of macroporosity on pedotransfer function estimates at the field scale. Vadose Zone J. 18.

Zhao, C., Shao, M.A., Jia, X., Nasir, M., Zhang, C., 2016. Using pedotransfer functions to estimate soil hydraulic conductivity in the Loess Plateau of China. CATENA 143, 1-6.